PRAMANA — journal of physics

Vol. 76, No. 3
March 2011
pp. 431–440

Cluster radioactivity leading to doubly magic ^{100}Sn and ^{132}Sn daughters

K P SANTHOSH
School of Pure and Applied Physics, Kannur University, Payyanur Campus, Payyanur 670 327, India
E-mail: drkpsanthosh@gmail.com

MS received 1 June 2010; revised 13 August 2010; accepted 8 September 2010

Abstract. Decay of neutron-deficient $^{128–137}$Gd parents emitting ^{4}He to ^{32}S clusters are studied within the Coulomb and proximity potential model. The predicted half-lives are compared with other models and most of the values are well within the present experimental limit for measurements ($T_{1/2} < 10^{30}$ s). The lowest $T_{1/2}$ value for ^{28}Si emission from ^{128}Gd indicates the role of doubly magic ^{100}Sn daughter in cluster decay process. It is also found that neutron excess in the parent nuclei slows down the cluster decay process. Geiger–Nuttal plots for all clusters are found to be linear with different slopes and intercepts. The α-decay half-lives of $^{148–152}$Gd parents are computed and are in agreement with experimental data. The role of doubly magic ^{132}Sn daughter in cluster decay process is also examined for various neutron-rich Ba, Ce, Nd, Sm and Gd parents emitting clusters ranging from ^{4}He to ^{32}Si. Alpha-like structures are most probable in the decays leading to ^{100}Sn, while non-α-like structures are probable in the decays leading to ^{132}Sn. The neutron–proton asymmetry in parent and daughter nuclei is responsible for the reduced decay rate in the decay leading to ^{132}Sn.

Keywords. Cluster radioactivity; alpha decay.

PACS Nos 23.70.+j; 23.60.+e

1. Introduction

The spontaneous decay of radioactive nuclei with the emission of cluster, heavier than alpha particle, without being accompanied by neutron emission, is termed as exotic decay or cluster radioactivity. Sandulescu *et al* [1] in 1980 predicted this phenomenon on the basis of quantum mechanical fragmentation theory (QMFT). Rose and Jones [2] in 1984 observed the first evidence of exotic decays and a few months later Alexandrov *et al* [3] observed it in the spontaneous emission of ^{14}C cluster from ^{223}Ra. About 24 modes of cluster decays from 18 parent nuclei, emitting clusters ranging from carbon to silicon, were so far confirmed. Upper limit for the decay rate for 16 modes were measured and

one case of fine structure in the energy spectrum of ^{14}C clusters from ^{223}Ra was found [4]. This phenomenon can be treated as a case of strong asymmetric fission [5] or an exotic process of cluster formation and tunnelling through the barrier making much assault on the barrier similar to α-decay [6].

The instability against exotic cluster decay of 'stable' nuclei was first pointed out by Gupta and collaborators [7] in 1989 and new instabilities against exotic decay of some stable nuclei in the region $Z = 50$–82 were pointed out by Gupta *et al* [8] in 1993. Based on the analytical super-asymmetric fission model (ASAFM), Poenaru *et al* [9] and based on preformed cluster model (PCM), Kumar and coworkers [10,11] calculated half-life for neutron-deficient parents with $Z = 56$–64 and $N = 58$–72 which decay by ^{4}He, ^{12}C, ^{16}O and ^{28}Si emissions. This region is very interesting because the daughter nuclei in such decays are formed around doubly magic ^{100}Sn and the estimated half-lives are below the present limit of measurements ($T_{1/2} < 10^{30}$ s). Moreover, only $N = Z$ clusters are emitted from this region and Z/A values for parent, daughter and emitted cluster are nearly equal to 0.5. Experiments for producing such parent nuclei, which lie far from beta stability line, were conducted at Dubna (Russia) [12,13] and at GSI, Dramstat (Germany) [14–16].

Taking interacting potential as the sum of Coulomb and proximity potentials, we have calculated the half-life for ^{12}C emission from various barium isotopes using different mass tables [17]. The predicted logarithmic half-life for ^{12}C emission from ^{112}Ba isotope was 3.78 s which is in good agreement with the value 3.75 s reported by Guglielmetti *et al* [15]. This result however could not be reproduced in the experiments [16] carried out at GSI in 1997. Hence, the above half-life values are taken as the experimental lower limit. In this work, we extended our studies to ^{4}He, ^{8}Be, ^{12}C, ^{16}O, ^{20}Ne, ^{24}Mg, ^{28}Si, ^{29}Si and ^{32}S emissions from various neutron-deficient $^{128-137}$Gd parents. The role of doubly magic ^{132}Sn daughter in cluster decay process is also examined for various neutron-rich Ba, Ce, Nd, Sm and Gd parents emitting clusters ranging from ^{4}He to ^{32}Si. The details of Coulomb and proximity potential models are given in §2 and results, discussion and conclusion are given in §3.

2. The Coulomb and proximity potential model

The interacting potential barrier for a parent nucleus exhibiting exotic decay is given by

$$V = \frac{Z_1 Z_2 e^2}{r} + V_{\mathrm{p}}(z) + \frac{\hbar^2 \ell(\ell+1)}{2\mu r^2}, \quad \text{for } z > 0. \tag{1}$$

Here Z_1 and Z_2 are the atomic numbers of daughter and emitted cluster, r is the distance between fragment centres, z is the distance between the near surfaces of the fragments, ℓ is the angular momentum, μ is the reduced mass and V_{p} is the proximity potential given by Blocki *et al* [18]

$$V_{\mathrm{p}}(z) = 4\pi\gamma b\left[\frac{C_1 C_2}{(C_1 + C_2)}\right]\Phi\left(\frac{z}{b}\right). \tag{2}$$

With the nuclear surface tension coefficient,

$$\gamma = 0.9517\left[1 - 1.7826\,(N-Z)^2/A^2\right]\ \mathrm{MeV/fm^2}, \tag{3}$$

where N, Z and A represent neutron, proton and mass number of the parent, Φ, the universal proximity potential is given as [19]

$$\Phi(\varepsilon) = -4.41\mathrm{e}^{-\varepsilon/0.7176}, \quad \text{for } \varepsilon \geq 1.9475 \tag{4}$$

$$\Phi(\varepsilon) = -1.7817 + 0.9270\varepsilon + 0.0169\varepsilon^2 - 0.05148\varepsilon^3, \quad \text{for } 0 \leq \varepsilon \leq 1.9475 \tag{5}$$

with $\varepsilon = z/b$, where the width (diffuseness) of the nuclear surface $b \approx 1$ and Siissmann central radii C_i of fragments related to sharp radii R_i is

$$C_i = R_i - \left(\frac{b^2}{R_i}\right). \tag{6}$$

For R_i we use semi-empirical formula in terms of mass number A_i as [18]

$$R_i = 1.28A_i^{1/3} - 0.76 + 0.8A_i^{-1/3}. \tag{7}$$

Using one-dimensional WKB approximation, the barrier penetrability P is given as

$$P = \exp\left\{-\frac{2}{\hbar}\int_a^b \sqrt{2\mu\,(V-Q)}\,\mathrm{d}z\right\}. \tag{8}$$

Here the mass parameter is replaced by $\mu = mA_1A_2/A$, where m is the nucleon mass and A_1, A_2 are the mass numbers of daughter and emitted cluster respectively. The turning points a and b are determined from the equation $V(a) = V(b) = Q$. The above integral can be evaluated numerically or analytically, and the half-life is given by

$$T_{1/2} = \left(\frac{\ln 2}{\lambda}\right) = \left(\frac{\ln 2}{\upsilon P}\right), \tag{9}$$

where $\upsilon = (\omega/2\pi) = (2E_v/h)$ represents the number of assaults on the barrier per second and λ is the decay constant. E_v, the empirical zero point vibration energy is given as [20]

$$E_v = Q\left\{0.056 + 0.039\exp\left[\frac{(4-A_2)}{2.5}\right]\right\}, \quad \text{for } A_2 \geq 4. \tag{10}$$

3. Results, discussion and conclusion

We have made our calculations taking potential energy as the sum of Coulomb and proximity potentials of Blocki *et al* [18,19] for the touching configuration and for the separated fragments. From touching configuration and down to parent central radius (overlap region), we used simple power-law interpolation. Proximity potential was first used by Shi and Swiatecki [21] in an empirical manner and has been quite extensively used

by Gupta and collaborators [22] for over a decade now in the preformed cluster model (PCM), which is based on the 'pocket formula' of Blocki *et al* [18] given as

$$\Phi(\varepsilon) = -\left(\frac{1}{2}\right)(\varepsilon - 2.54)^2 - 0.0852\,(\varepsilon - 2.54)^3\,, \quad \text{for } \varepsilon \leq 1.2511, \tag{11}$$

$$\Phi(\varepsilon) = -3.437\exp\left(\frac{-\varepsilon}{0.75}\right), \quad \text{for } \varepsilon \geq 1.2511. \tag{12}$$

In the present model, another formulation of proximity potential [19] given by eqs (4) and (5) has been used. Inclusion of proximity potential reduces the height of potential barrier which closely agrees with experimental value. For calculating decay constant, we have taken preformation probability as unity for all clusters irrespective of their masses. The present model differs from PCM by a factor P_0, the preformation probability. In our model, contribution of both internal and external parts of the barrier is considered for the penetrability calculation, but in PCM only the external part of the barrier is taken into consideration. In the present model, assault frequency υ is calculated for each parent–cluster combination, which is associated with zero point vibration energy. For zero point vibration energy E_v, we used the semi-empirical formula of Poenaru *et al* [20]. We would like to mention that according to Poenaru *et al* [23,24], a realistic preformation factor can be calculated within the fission model as the penetrability of the internal part (overlap region) of the barrier.

In the present work the cluster decay calculations were done by assuming zero angular momentum transfers, because the angular momentum ℓ carried away in the cluster decay process, appearing in eq. (1) is very small ($\approx 5/\hbar$) and its contribution to half-life is shown to be small [20] which is decided by the spin-parity conservation. Table 1 gives the logarithm of the predicted half-life for ^{4}He, ^{8}Be, ^{12}C, ^{16}O, ^{20}Ne, ^{24}Mg, ^{28}Si, ^{29}Si and ^{32}S clusters from $^{128-137}$Gd isotopes using different mass tables and their comparison with other models [9,11,25]. It is found that most of the values are below the present upper limit for measurements ($T_{1/2} < 10^{30}$ s) and our values are closer to those values reported by ASAFM [25]. In our model the penetration of the barrier by the cluster is a direct penetration, and therefore full contribution of the barrier (both internal and external) is taken into account in the penetrability calculation. In PCM the penetration is step-wise, the cluster first penetrates from touching point R_t to R_i, gets de-excited and then penetrates from R_i to outer turning point R_b (see figure 1 of ref. [22]), and as a result full contribution of the external barrier does not appear in the penetrability calculation. This is the reason for the deviation of our prediction from that of PCM.

It is found that ^{28}Si emissions from ^{128}Gd and ^{130}Gd are most favourable for measurement with the smallest half-life values ($T_{1/2} \leq 10^{17}$ s). The lowest $T_{1/2}$ value for ^{28}Si emission from ^{128}Gd indicates the role of doubly magic ^{100}Sn daughter in cluster decay process and in the case of ^{28}Si from ^{130}Gd, the daughter is ^{102}Sn which lies close to $N = Z = 50$ shell. The nuclei considered in the present paper are at the extreme end of the proton-rich side, the estimated branching ratios with respect to α-decay for ^{28}Si emissions from ^{128}Gd and ^{130}Gd are 2.113×10^{-8} and 8.793×10^{-14}, respectively and are measurable in an on-line experiment. We would like to point out that the branching ratio with respect to α-decay, as low as 10^{-18}, has already been measured [4]. Radioactive beams can be used to produce these nuclei far from β stability line.

Table 1. Logarithm of predicted half-lives and other characteristics of various Gd parents emitting ^{4}He, ^{8}Be, ^{12}C, ^{16}O, ^{20}Ne, ^{24}Mg, ^{28}Si, ^{29}Si and ^{32}S clusters and comparison with other models [9,11,25]. $T_{1/2}$ is in seconds.

Parent	Emitted	Daughter	Q value	Penetrability	Decay	$\log_{10}(T_{1/2})$		
nuclei	cluster	nuclei	(MeV)	P	constant	Present	ASAFM	PCM
^{128}Gd	^{4}He	^{124}Sm	3.70	1.467E-28	2.494E-08	7.44		3.28
^{130}Gd		^{126}Sm	4.16	2.354E-25	4.498E-05	4.19		1.55
^{132}Gd		^{128}Sm	3.90	5.676E-27	1.017E-06	5.83	5.40	3.76
			3.58	2.622E-29	4.312E-09	8.21	7.60	
			3.70	2.137E-28	3.632E-08	7.28	6.80	
^{133}Gd		^{129}Sm	3.85	2.791E-27	4.936E-07	6.15	6.60	
			3.82	1.718E-27	3.015E-07	6.36	6.70	
^{134}Gd		^{130}Sm	3.80	1.347E-27	2.352E-07	6.47	6.10	
			3.87	4.177E-27	7.426E-07	5.97	5.70	
			3.96	1.712E-26	3.115E-06	5.35	5.00	
^{135}Gd		^{131}Sm	3.67	1.639E-28	2.764E-08	7.40	8.10	
			3.57	2.813E-29	4.614E-09	8.18	8.80	
			3.70	2.743E-28	4.663E-08	7.17	7.90	
^{136}Gd		^{132}Sm	4.37	7.182E-24	1.442E-03	2.68	2.50	
			3.46	4.009E-30	6.374E-10	9.04	8.70	
			3.57	3.041E-29	4.988E-09	8.14	7.90	
^{137}Gd		^{133}Sm	3.83	2.774E-27	4.882E-07	6.15	7.10	
^{128}Gd	^{8}Be	^{120}Nd	6.12	3.343E-65	6.320E-45	44.04		30.54
^{130}Gd		^{122}Nd	6.37	9.349E-63	1.840E-42	41.58		26.99
^{132}Gd		^{124}Nd	6.65	3.386E-60	6.954E-40	39.00		25.47
^{137}Gd		^{129}Nd	8.94	1.416E-44	3.909E-24	23.25	23.00	
^{128}Gd	^{12}C	^{116}Ce	17.51	1.499E-47	7.314E-27	25.98		14.65
^{130}Gd		^{118}Ce	16.50	5.811E-51	2.671E-30	29.41		17.66
^{132}Gd		^{120}Ce	16.19	6.536E-52	2.947E-31	30.37		18.16
^{136}Gd		^{124}Ce	17.99	6.129E-45	3.071E-24	23.35	21.90	
^{137}Gd		^{125}Ce	17.09	5.602E-48	2.666E-27	26.41	26.30	
^{128}Gd	^{16}O	^{112}Ba	28.67	1.138E-44	8.889E-24	22.89		14.63
^{130}Gd		^{114}Ba	27.18	3.429E-48	2.539E-27	26.44		16.96
^{132}Gd		^{116}Ba	25.84	1.312E-51	9.231E-31	29.88		19.20
^{128}Gd	^{20}Ne	^{108}Xe	36.78	5.591E-50	5.576E-29	28.09		21.37
^{130}Gd		^{110}Xe	35.44	1.009E-52	9.696E-32	30.58		23.20
^{132}Gd		^{112}Xe	33.36	1.309E-57	1.184E-36	35.77		26.40

Table 1. *Continued.*

Parent	Emitted	Daughter	Q value	Penetrability	Decay	$\log_{10}(T_{1/2})$		
nuclei	cluster	nuclei	(MeV)	P	constant	Present	ASAFM	PCM
^{128}Gd	^{24}Mg	^{104}Te	50.02	2.704E-43	3.664E-22	21.28		18.99
^{130}Gd		^{106}Te	48.48	9.649E-46	1.267E-24	23.74		21.54
^{132}Gd		^{108}Te	46.57	3.941E-49	4.971E-28	27.14		24.31
^{128}Gd	^{28}Si	^{100}Sn	63.03	3.086E-37	5.269E-16	15.12		12.01
^{130}Gd		^{102}Sn	61.42	2.378E-39	3.955E-18	17.24		15.08
^{132}Gd		^{104}Sn	59.62	6.104E-42	9.711E-21	19.85		17.95
			59.28	1.415E-42	2.272E-21	20.48	20.60	
			59.42	2.569E-42	4.136E-21	20.22	20.40	
^{133}Gd		^{105}Sn	58.15	2.229E-44	3.509E-23	22.30	23.50	
			57.75	3.877E-45	6.064E-24	23.06	24.10	
			58.06	1.505E-44	2.367E-23	22.47	23.60	
^{134}Gd		^{106}Sn	56.94	2.150E-46	3.314E-25	24.32	23.90	
			57.07	3.834E-46	5.926E-25	24.07	23.70	
			57.09	4.191E-46	6.479E-25	24.03	23.70	
^{135}Gd		^{107}Sn	55.48	5.638E-49	8.472E-28	26.91	27.40	
			55.87	3.355E-48	5.076E-27	26.14	26.80	
^{136}Gd		^{108}Sn	54.50	1.127E-50	1.664E-29	28.62	27.60	
			54.82	5.025E-50	7.461E-29	27.97	27.10	
^{133}Gd	^{29}Si	^{104}Sn	56.99	1.971E-46	3.042E-25	24.36	25.90	
			56.60	3.364E-47	5.157E-26	25.13	26.50	
			56.90	1.312E-46	2.022E-25	24.53	26.00	
^{135}Gd		^{106}Sn	55.26	2.703E-49	4.045E-28	27.23	28.50	
			55.69	1.666E-48	2.511E-27	26.44	27.80	
^{132}Gd	^{32}S	^{100}Cd	66.45	2.553E-45	4.595E-24	23.18	23.10	
			64.19	1.573E-49	2.734E-28	27.40	26.40	
			66.59	4.609E-45	8.312E-24	22.92	22.90	
^{133}Gd		^{101}Cd	65.10	1.856E-47	3.273E-26	25.33	26.00	
			64.70	3.329E-48	5.770E-27	26.08	26.60	

When decay of ^{28}Si from ^{128}Gd is compared with that from heavier isotopes up to ^{136}Gd, it is found that $\log_{10}(T_{1/2})$ value increases from 15.12 s (for ^{128}Gd, $Q = 63.03$ MeV) to 28.62 s (for ^{136}Gd, $Q = 54.50$ MeV). All these cases refer to the doubly magic or near doubly magic daughter ^{100}Sn nuclei. This result points to the fact that the neutron excess in the parent nuclei slows down the exotic decay process.

Figure 1 gives the Geiger–Nuttal plots of the predicted $\log_{10}(T_{1/2})$ vs. $Q^{-1/2}$ for ^{4}He, ^{8}Be, ^{12}C, ^{16}O, ^{20}Ne, ^{24}Mg, ^{28}Si and ^{32}S from various Gd isotopes. We notice that the

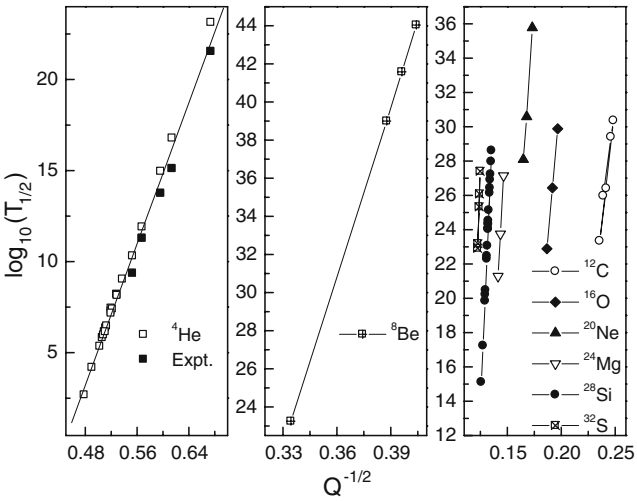

Figure 1. Geiger–Nuttal plot for $\log_{10}(T_{1/2})$ vs. $Q^{-1/2}$ for cluster emission from various Gd parents.

Geiger–Nuttal plots for all clusters are linear with different slopes and intercepts. The difference in slope and intercept of Geiger–Nuttal plots arises due to shell effect (through Q value). We would like to point out that the Geiger–Nuttal plot is for pure Coulomb potential but from our study it is clear that inclusion of the proximity potential will not affect its linear nature. The α-decay half-lives of $^{148-152}$Gd parents (for which experimental data [26] are available) are also computed and are in good agreement with each other,

Table 2. Logarithm of predicted half-lives and other characteristics of parent nuclei which decay to ^{132}Sn daughter. $T_{1/2}$ is in seconds.

Parent nuclei	Emitted cluster	Q value (MeV)	Penetrability P	Decay constant	$\log_{10}(T_{1/2})$
^{144}Ba	^{12}C	5.49	7.7577E-115	1.1862E-94	93.77
^{146}Ba	^{14}C	8.13	3.2649E-86	7.2803E-66	64.98
^{148}Ce	^{16}O	10.66	5.6769E-111	1.6483E-90	89.62
^{152}Ce	^{20}O	14.81	4.3078E-85	1.7298E-64	63.60
^{152}Nd	^{20}Ne	13.83	1.0210E-133	3.8287E-113	112.26
^{156}Nd	^{24}Ne	23.34	9.2285E-80	5.8347E-59	58.07
^{156}Sm	^{24}Mg	20.96	7.3216E-128	4.1570E-107	106.22
^{160}Sm	^{28}Mg	31.41	1.3768E-81	1.1712E-60	59.77
^{160}Gd	^{28}Si	30.55	4.9152E-117	4.0669E-96	95.23
^{164}Gd	^{32}Si	40.80	6.4931E-81	7.1746E-60	58.98

Table 3. Logarithm of predicted half-lives and other characteristics of parent nuclei which decay to ^{100}Sn and their comparison with PCM [10,11]. $T_{1/2}$ is in seconds.

Parent nuclei	Emitted cluster	Q value (MeV)	Penetrability P	Decay constant	$\log_{10}(T_{1/2})$ Present	PCM
^{112}Ba	^{12}C	21.64	1.92605E-25	1.15120E-04	3.78	3.75
^{116}Ce	^{16}O	31.71	6.12654E-28	5.29147E-07	6.12	6.14
^{120}Nd	^{20}Ne	39.41	4.80487E-36	5.13421E-15	14.13	17.04
^{124}Sm	^{24}Mg	49.70	3.36335E-39	4.52807E-18	17.18	17.32
^{128}Gd	^{28}Si	63.03	3.08642E-37	5.26874E-16	15.12	12.01

and both of them lie on the Geiger–Nuttal plot. That is, for ^{149}Gd parent, $T_{1/2}^{\text{Expt}} = 11.28$; $T_{1/2}^{\text{Present}} = 11.91$.

3.1 *Decay leading to ^{132}Sn*

To examine the role of doubly magic ^{132}Sn in exotic decay process, the exotic decay of neutron-rich $^{144-152}$Ba, $^{148-156}$Ce, $^{152-160}$Nd, $^{156-164}$Sm and $^{160-168}$Gd parents emitting clusters ranging from ^{4}He to ^{32}Si are studied. The Q value estimates show that these parents are stable against ^{4}He, ^{8}Be and ^{10}Be emissions ($Q < 0$). For ^{4}He emission, ^{144,146}Ba, ^{148,150}Ce, ^{152}Nd, ^{156,158}Sm, ^{162,164,166}Gd isotopes have positive Q values but the computed $T_{1/2}$ values show that these nuclei are stable against α-decay ($T_{1/2} > 10^{40}$ s). From our study it is clear that the decays of ^{14}C from ^{146}Ba, ^{20}O from ^{152}Ce, ^{24}Ne from ^{156}Nd, ^{28}Mg from ^{160}Sm and ^{32}Si from ^{160}Gd have the lowest $T_{1/2}$ value compared to the decay from

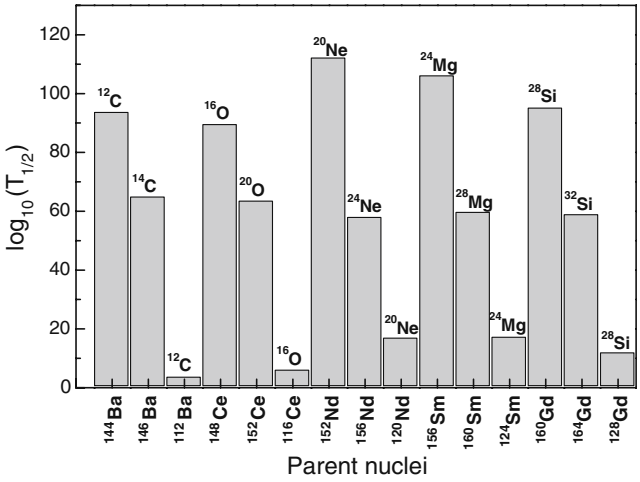

Figure 2. Histogram showing half-lives for various cluster emissions from neutron-rich and neutron-deficient parents.

neighbouring ones. All these decays lead to doubly magic ^{132}Sn daughter. Table 2 gives the logarithm of the predicted half-life and other characteristics of neutron-rich Ba–Gd parents which decay to ^{132}Sn daughter and table 3 gives that for neutron-deficient parents which decay to doubly magic ^{100}Sn daughter.

Figure 2 gives the comparison of half-lives for various cluster emissions from both neutron-rich and neutron-deficient parents. It is found that carbon emissions from ^{144}Ba and ^{146}Ba have $T_{1/2}$ values larger than that of ^{112}Ba. Here both the cases refer to doubly magic ^{132}Sn and ^{100}Sn daughter respectively. Same is the case for oxygen emission from Ce isotopes, Ne emission from Nd isotopes, Mg emission from Sm isotopes and Si emission from Gd isotopes. It is evident that the decay leading to ^{100}Sn is most probable for measurements ($T_{1/2} \leq 10^{17}$ s). The neutron–proton asymmetry in parent and daughter nuclei is responsible for the reduced decay rate in the case of decay leading to ^{132}Sn. The preference of non-α-like structure in decays leading to ^{132}Sn and α-like structure in the decays leading to ^{100}Sn, point out the importance of asymmetry and symmetry of proton–neutron in the two cases. We would like to mention that non-α-like structures (i.e. ^{14}C, ^{20}O, ^{24}Ne, ^{28}Mg and ^{34}Si) have already been observed [4] in the cluster decays of various parents leading to ^{208}Pb daughter.

References

[1] A Sandulescu, D N Poenaru and W Greiner, *Sov. J. Part. Nucl.* **II**, 528 (1980)
[2] H J Rose and G A Jones, *Nature* **307**, 245 (1984)
[3] D V Alexandrov, A F Belyatsky, Yu A Glukhov, Yu E Nikolsky, B V Novatsky, A A Ogloblin and D N Stepanov, *JEPT Lett.* **40**, 909 (1984)
[4] R Bonetti and A Guglielmetti, *Heavy elements and related new phenomena* edited by W Greiner and R K Gupta (World Scientific, Singapore, 1999) Vol. 2, p. 643
[5] D N Poenaru, M Ivascu and A Sandulescu, *J. Phys. G: Nucl. Part. Phys.* **5**, L169 (1979)
[6] R Blendowske, T Fliessbach and H Walliser, *Nucl. Phys.* **A464**, 75 (1987)
[7] S S Malik, S Singh, R K Puri, S Kumar and R K Gupta, *Pramana – J. Phys.* **32**, 419 (1989)
[8] R K Gupta, S Singh, R K Puri and W Schied, *Phys. Rev.* **C47**, 561 (1993)
[9] D N Poenaru, W Greiner and R Gherghescu, *Phys. Rev.* **C47**, 2030 (1993)
[10] S Kumar and R K Gupta, *Phys. Rev.* **C49**, 1922 (1994)
[11] S Kumar, D Bir and R K Gupta, *Phys. Rev.* **C51**, 1762 (1995)
[12] Yu Ts Oganessian, V L Mikheev and S P Tretyakova, *JINR Dubna Report No. E 7-93-57* (1993)
[13] Yu Ts Oganessian, A Lazarev, V L Mikheev, Yu A Shirokovsy, S P Tretyakova and V K Utyonkov, *Z. Phys.* **A349**, 341 (1994)
[14] A Guglielmetti, R Bonetti, G Poli, P B Price, A J Westphal, Z Janas, H Keller, R Kirchner, O Klepper, A Piechaczek, E Roeckl, K Schmidt, A Plochocki, J Szeryo and B Blank, *Phys. Rev.* **C52**, 740 (1995)
[15] A Guglielmetti, B Blank, R Bonetti, Z Janas, H Keller, R Kirchner, O Klepper, A Piechaczek, A Plochocki, G Poli, P B Price, E Roeckl, K Schmidt, J Szeryo and A J Westphal, *Nucl. Phys.* **A583**, 867c (1995)
[16] A Guglielmetti, R Bonetti, G Poli, R Collatz, Z Hu, R Kirchner, E Roeckl, N Gunn, P B Price, B A Weaver and A J Westphal, *Phys. Rev.* **C56**, R2912 (1997)
[17] K P Santhosh and A Joseph, *Pramana – J. Phys.* **55**, 375 (2000)
[18] J Blocki, J Randrup, W J Swiatecki and C F Tsang, *Ann. Phys (N.Y.)* **105**, 427 (1977)

[19] J Blocki and W J Swiatecki, *Ann. Phys (N.Y.)* **132**, 53 (1981)
[20] D N Poenaru, M Ivascu, A Sandulescu and W Greiner, *Phys. Rev.* **C32**, 572 (1985)
[21] Y J Shi and W J Swiatecki, *Nucl. Phys.* **A438**, 450 (1985)
[22] S S Malik and R K Gupta, *Phys. Rev.* **C39**, 1992 (1989)
[23] D N Poenaru and W Greiner, *J. Phys. G: Nucl. Part. Phys.* **17**, S443 (1991)
[24] D N Poenaru, W Greiner and E Hourani, *Phys. Rev.* **C51**, 594 (1995)
[25] D N Poenaru, D Schnabel, W Greiner, D Mazilu and R Gherghescu, *At. Data Nucl. Data Tables* **48**, 23 (1991)
[26] G Royer, *J. Phys. G: Nucl. Part. Phys.* **26**, 1149 (2000)